*Transactions of the Korean Nuclear Society Autumn Meeting*
*Yeosu, Korea, October 25-26, 2018*

# Combined Effects of Magnetite and Sulfur Oxyanions on the Corrosion Behavior of Alloy 600

Jeoh Han[a,b], Geun Dong Song[a], Soon-Hyeok Jeon[a], Jong Hyeon Lee[b], Do Haeng Hur[a,*]
[a] *Nuclear Materials Research Division, Korea Atomic Energy Research Institute, 989-111 Daedeok-daero, Yuseong-gu, Daejeon, 34057, Republic of Korea*
[b] *Department of Advanced Materials Engineering, Chungnam National University, 99 Daehak-ro, Yuseong-gu, Daejeon, 34134, Republic of Korea*
[*]Corresponding author: dhhur@kaeri.re.kr

## 1. Introduction

Alloy 600 has been used as a tubing material of steam generators (SG) in pressurized water reactors (PWR). The stress corrosion cracking (SCC) of Alloy 600 SG tubing has been a major degradation mode in PWRs [1-2]. Therefore, lots of laboratories have studied on the secondary side SCC of Alloy 600 in solutions containing various impurities and pH conditions [3-4]. However, it should be considered that the outer surface of the tubing is covered with magnetite deposit, which is released from carbon steel piping and transported into the SGs in operation. The magnetite deposit contains numerous pores, called boiling chimneys [5], which are formed when steam bubbles are departed from the SG tube surface. Thus, some chemical impurities like sulfur oxyanions, lead, and chloride ions can be concentrated within the pores in this process. These phenomena accelerate the corrosion of the SG tubing [6-7]. This means that actual corrosion phenomena can occur under conditions wherein the local surface of a tube is in contact with porous magnetite deposits.

Among many of the impurities, sulfur can be originated from feed water and resin beads [8]. Sulfur can exist in many valence states, such as − 2 ($S^{2-}$), +2 ($S_2O_3^{2-}$), +2.5 ($S_4O_6^{2-}$) and +6 ($SO_4^{2-}$). Reduced forms of sulfur could be generated by reaction of sulfate ion with hydrazine during SG operation and they can cause IGA and pitting of high-nickel alloys like Alloy 600 [9-10].

Recently, we have reported that the general corrosion of carbon steel and Ni-based alloys is significantly accelerated by a galvanic effect between the materials and magnetite in various simulated secondary environments [11-15]. However, the effect of sulfur oxyanions has not been considered in evaluating the effect of magnetite on the stress corrosion cracking behavior of Alloy 600 until now.

The objective of this research is to assess the combined effect of sulfur oxyanions (sulfate and tetrathionate) and magnetite on the SCC behavior of Alloy 600. In order to investigate SCC behavior of Alloy 600 coupled with magnetite, two types of SCC specimen (Alloy 600 uncoupled and coupled with electrodeposited magnetite) were prepared and tested in sulfur oxyanion-containing solutions at 340 ℃. Electrochemical tests were also conducted to evaluate the corrosion behavior of Alloy 600 and magnetite at 80 ℃.

## 2. Experimental Methods

### *2.1. ZRA tests*

To evaluate the galvanic corrosion behavior of Alloy 600 and magnetite, zero resistance ammetry (ZRA) tests were conducted at 80 ℃. A reference solution of pH 9.0 at 25 ℃ was prepared using NaOH as a pH adjuster, and 1 M $Na_2SO_4$ were added to the reference solution. The area ratio between Alloy 600 and magnetite specimen was 1:10. A saturated calomel electrode was used as a reference electrode. Alloy 600 specimen was connected to the working electrode and magnetite specimen was connected to the counter electrode. The test solution was deaerated by purging high purity nitrogen gas (99.999 %) at a rate of 100 $cm^3$/min until the test was over.

### *2.2. Preparation of U-bend specimens*

A type of U-bend specimen was used for SCC tests. Mill-annealed Alloy 600 plates with a size of 24.4 mm x 7 mm x 1.25 mm were ground with SiC papers up to 600 grit and ultrasonically cleaned in acetone. Each plate was bended using a bending jig, and the legs of the U-bend specimen were fastened to be parallel to each other using a bolt and nut made of Alloy 600 material, as shown in Fig. 1(a).

To evaluate the effect of magnetite on the SCC behavior of Alloy 600, the SCC specimen must be in contact with magnetite in the test solution. To attain this condition, a magnetite layer was electrodeposited over the whole surface of the assembled U-bend specimen except the apex area of approximately 0.5 mm width. The electrodeposition solution consisted of 2 M NaOH, 0.1 M triethanolamine and 0.043 M $Fe_2(SO_4)_3$. The electrodeposition of magnetite layer was conducted at an applied potential of $-1.05\ V_{SCE}$ for 30 minutes at 80 ℃. The magnetite-depostited U-bend specimen is shown in Fig. 1(b). In this paper, the magnetite-free specimens and the magnetite-deposited specimens are referred to as uncoupled and coupled specimens, respectively.

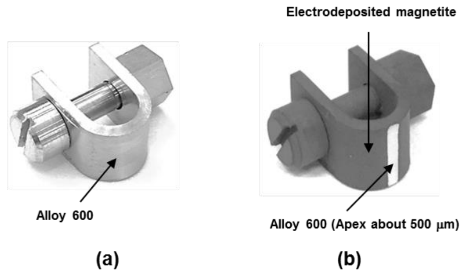

Fig. 1. Photographs of U-bend specimens: (a) uncoupled U-bend, and (b) coupled U-bend.

### *2.3. SCC tests*

The SCC tests were conducted in sulfur oxyanions-containing solutions at 340 ℃. To evaluate the effect of sulfur oxyanions on the SCC behavior of Alloy 600, two types of test solution were prepared. A reference solution of pH 9.0 at 25 ℃ was first prepared using NaOH as a pH adjuster, and then added 0.05 M $Na_2SO_4$. The other test solution was prepared by adding 0.05 M $Na_2SO_4$ and 0.01 M $Na_2S_4O_6$ to the reference solution. Each solution of 2 L was poured into an autoclave and deaerated by blowing high purity argon gas with a flow rate of 300 ml/min in the closed autoclave for 3 hours. The test was interrupted to examine the U-bend specimens every 500 h and the test solution was changed every 500 h for the successive test.

## 3. Results and Discussions

Fig. 2 shows the variation of the corrosion potentials of the test materials in 1 M $Na_2SO_4$ solution at 80 ℃. The dotted black line is the corrosion potential of Alloy 600 and the dotted red line is the corrosion potential of magnetite when they are in the open circuit. However, when two materials were connected in an area ratio of 1:10, the corrosion potential (blue line) of Alloy 600 was raised up to that of magnetite. This result indicates that Alloy 600 becomes the anode of the galvanic couple with magnetite and its corrosion rate would be increased when two materials are galvanically coupled.

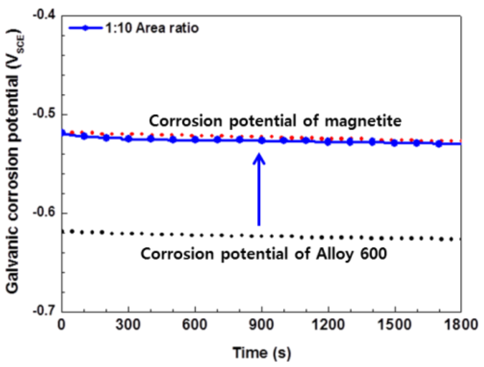

Fig. 2. Change of the corrosion potentials of Alloy 600 uncoupled and coupled with magnetite in 1 M $Na_2SO_4$ solution at 80 ℃.

Fig. 3 shows the comparison of galvanic corrosion current of Alloy 600 coupled with magnetite in an area ratio of 1:10 in both the reference solution and 1 M $Na_2SO_4$ solution. The corrosion current of Alloy 600 galvanically connected with magnetite showed the anodic current. This confirms that Alloy 600 behaves as an anode when Alloy 600 and magnetite are electrically connected. The galvanic current density of Alloy 600 was increased by about 5-times in the sulfate solution than in the reference solution.

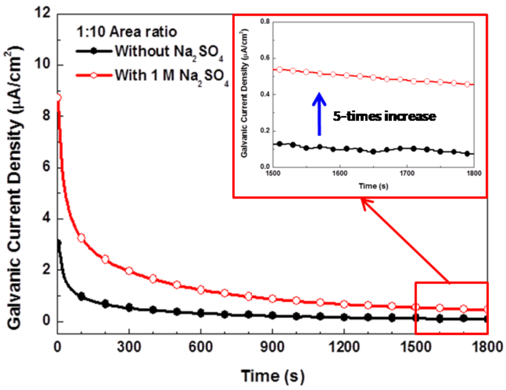

Fig. 3 Comparison of galvanic current density of Alloy 600 in reference solution and sulfate solution at 80 ℃.

Fig. 4 shows the optical microscope (OM) images of U-bend specimens after the SCC tests in sulfate (0.05 M $Na_2SO_4$) and mixed sulfur oxyanions (0.05 M $Na_2SO_4$ + 0.01 M $Na_2S_4O_6$) solution. Fig. 4 (a) is the top-view image of the U-bend specimen before the SCC test, (b) is the image after the SCC test in 0.05 M $Na_2SO_4$ solution for 1500 h, and (c) is the image after the SCC test in 0.05 M $Na_2SO_4$ + 0.01 M $Na_2S_4O_6$ solution for 500 h. The appearance of the U-bend specimens before test and after 1500 h test in the 0.05 M $Na_2SO_4$ solution was very similar to each other except for the color change of the exposed base alloy near apex from metallic color to dark yellow color due to oxidation of base metal. However, in the mixed sulfur oxyanions, it was observed that the entire surface of the specimen was highly corroded, resulting in the formation of a thick corrosion product layer on the specimen surface.

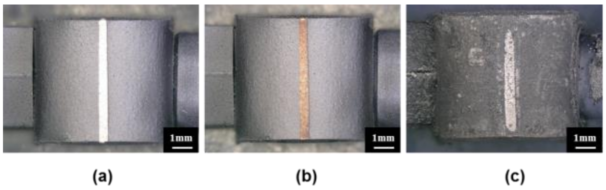

Fig. 4. OM images of U-bend specimens: (a) before the test, (b) after 1500 h test in 0.05 M $Na_2SO_4$ solution at 340 ℃, and (c) after 500 h test in 0.05 M $Na_2SO_4$ + 0.01 M $Na_2S_4O_6$ solution at 340 ℃.

Fig. 5 shows the cross-sectional image of the U-bend specimen after 500 h SCC test in 0.05 M $Na_2SO_4$ + 0.01 $Na_2S_4O_6$ solution at 340 ℃. The surface of the specimen was irregularly corroded and damaged, and thick corrosion products adhered on the corroded surface. Some microscopic cracks were also observed beneath the damaged surface. On the other hand, any cracks could not be found in the solution containing only sulfate even after 1500 h test.

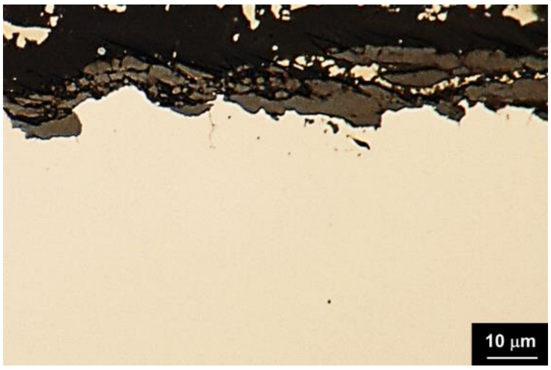

Fig. 5. Cross-section image of the U-bend specimen after 500 h test in 0.05 M $Na_2SO_4$ + 0.01 M $Na_2S_4O_6$ solution at 340 ℃.

Fig. 6 shows the cross-sectional image of the Alloy 600 and Alloy 600 coupled with magnetite after 500 h test. When the magnetite coupled to Alloy 600, it was observed that the surface of Alloy 600 was more corroded and damaged. In the case of the uncoupled Alloy 600, corrosion product was formed about 200 μm on the Alloy 600, but corrosion product of Alloy 600 coupled with magnetite was more accumulate than uncoupled specimen. This means that the general corrosion of Alloy 600 was accelerated by combining with magnetite in mixed sulfur oxyanions solution.

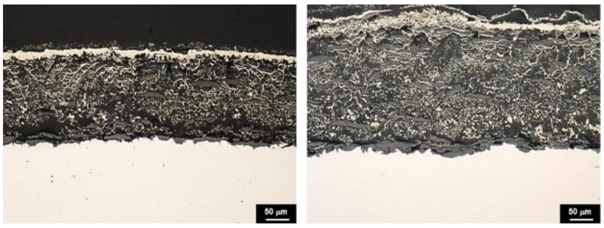

(a) (b)

Fig. 6. Corrosion product comparison of the U-bend specimen after 500 h test in 0.05 M $Na_2SO_4$ + 0.01 M $Na_2S_4O_6$ solution at 340 ℃:(a) Uncoupled, (b) Coupled U-bend specimen.

## 4. Conclusions

ZRA and SCC tests were conducted to investigate the corrosion behavior of Alloy 600 and magnetite in reference solution and sulfur oxyanions solution. The tentative conclusions can be drawn as follows.

(1) From the result of the ZRA tests, the galvanic current density of Alloy 600 coupled with magnetite was increased by about 5-times in the solution containing sulfate, compared to that in the reference solution.

(2) The general corrosion and SCC of Alloy 600 coupled with magnetite was more accelerated in the mixed solution of sulfate and tetrathionate, compared to those in the sulfate solution at 340 ℃.

## ACKNOWLEDGEMENTS

This work was supported by the National Research Foundation of Korea (NRF) grant funded by the Korea government (2017M2A8A4015159).

## REFERENCES

[1] R.B. Rebak, Z. Szklarska-smialowska, The Mechanism of Stress Corrosion Cracking of Alloy 600 in High Temperature Water, Corrosion Science, Vol. 38, No. 6, pp. 971-988, 1996.
[2] J. Panter, B. Viguier, J-M. Cloue, M. Foucault, P. Combrade, E. Andrieu, Influence of Oxide Films on Primary Water Stress Corrosion Cracking Initiation of Alloy 600, Journal of Nuclear Materials, 348, pp. 213-221, 2006.
[3] S.S. Hsu, S.C. Tsai, J.J. Kai, C.H. Tsai, SCC Behavior and Anodic Dissolution of Inconel 600 in Low Concentration Thiosulfate, Journal of Nuclear Materials, 184, pp. 97-106, 1991.
[4] E.A. Ashour, K. Mummert, H.J. Klau, Stress Corrosion Cracking of Inconel 600 in Aqueous Solution at Elevated Temperature, Materials and Corrosion, 48, pp. 151-156, 1997.
[5] S.H. Jeon, S. Hong, H.C. Kwon, D.H. Hur, Characteristics of steam generator tube deposits in an operating pressurized water reactor, Journal of Nuclear Materials, 507, pp. 371–380, 2018.
[6] R.L. Tapping, C.W. Turner, R.H. Thompson, Steam Generator Deposits – A Detailed Analysis and Some Inferences, Corrosion, Vol. 47, No. 6, pp. 489-495, 1991.
[7] R.W. Staehle, J.A. Gorman, Quantitative Assessment of Submodes of Stress Corrosion Cracking on the Secondary Side of Steam Generator Tubing in Pressurized Water Reactors, Corrosion, Vol. 59, No. 11, pp. 931-994, 2003.
[8] I.J Yang, Effect Sulphate and Chloride ions on the Crevice Chemistry and Stress Corrosion Cracking of Alloy 600 in High Temperature Aqueous Solutions, Corrosion Science, Vol. 33, No. 1, pp. 25-37, 1992.
[9] EPRI, Laboratory Program to Examine Effects of Layup Conditions on Pitting of Alloy 600, Research Project S124-1 Final Report NP-3012, 1983.
[10] EPRI, Pressurized Water Reactor Secondary Water Chemistry Guidelines – Revision 7, pp. 197, 2009.
[11] G.D. Song, S.H. Jeon, J.G. Kim, D.H. Hur, Effect of Polyacrylic Acid on the Corrosion Behavior of Carbon Steel and Magnetite in Alkaline Aqueous Solutions, Corrosion, 72, pp. 1010-1120, 2016.

[12] S.H. Jeon, G.D. Song, D.H. Hur, Corrosion Behavior of Alloy 600 Coupled with Electrodeposited Magnetite in Simulated Secondary Water of PWRs, Mater. Trans. 56, pp. 2078-2083, 2015.

[13] S.H. Jeon, G.D. Song, D.H. Hur, Electrodeposition of Magnetite on Carbon Steel in Fe(III)-Triethanolamine Solution and Its Corrosion Behavior, Mater. Trans. 56, pp. 1107-1111, 2015.

[14] S.H. Jeon, G.D. Song, D.H. Hur, Galvanic Corrosion Between Alloy 690 and Magnetite in Alkaline Aqueous Solutions, Metals, 5, pp. 2372-2382, 2015.

[15] G.D. Song, S.H. Jeon, J.G. Kim, D.H. Hur, Corrosion Science, Galvanic Effect of Magnetite on the Corrosion Behavior of Carbon Steel in Deaerated Alkaline Solutions under Flowing Conditions, Corrosion Science, 131, pp. 71-80, 2018.